Available online at www.sciencedirect.com
ScienceDirect
Journal of Power Sources 179 (2008) 830–836
JOURNAL OF POWER SOURCES
www.elsevier.com/locate/jpowsour

Evidence for electronic and ionic limitations at the origin of the second voltage plateau in nickel electrodes, as deduced from impedance spectroscopy measurements

F. Bardé [a], P.L. Taberna [b], J.M. Tarascon [a], M.R. Palacín [c,*]

[a] *Laboratoire de Réactivité et de Chimie des Solides, Université de Picardie Jules Verne, CNRS UMR 6007, F-80039 Amiens, France*
[b] *CIRIMAT, CNRS UMR 5085, Université Paul Sabatier, F-31062 Toulouse, France*
[c] *Institut de Ciència de Materials de Barcelona (CSIC), Campus UAB, E-08193 Bellaterra, Catalonia, Spain*

Received 9 September 2007; received in revised form 29 November 2007; accepted 19 January 2008
Available online 2 February 2008

Abstract

The second plateau occurring during the reduction of the nickel oxyhydroxide electrode (NOE) was studied by impedance spectroscopy on a cell with a pasted electrode prepared from commercial undoped β-$Ni(OH)_2$. Measurements were performed at diverse states of reduction and a large variation of impedance upon the transition from the first to the second plateau was observed. This variation mainly takes place at low frequencies and is hence related to ionic diffusion. We observed that the impedance becomes more capacitive on the second plateau meaning that the proton diffusion is limited. These results would be consistent with the gradual formation of an insulating layer of nickel hydroxide at the interface between the NOE and the electrolyte upon reduction. Once this layer becomes compact the ionic diffusion would be hindered and forced to occur through this layer, which could explain the voltage drop observed.

Keywords: Nickel batteries; Nickel hydroxide; Second plateau; Impedance spectroscopy

1. Introduction

Nickel-based alkaline batteries (Ni/Cd, Ni/MH or Ni/H_2) are well established in the market and widely used for very diverse applications including, among others, portable electronics, hybrid vehicles or space applications. Since the first patents by Jungner (Ni/Cd) [1,2] and Edison (Ni/Fe) [3,4], the positive nickel oxyhydroxide electrode (NOE) present in these batteries has been in use for more than a century. However, its development has often relied on empirical criteria and even though many studies have been devoted to the NOE our understanding of its redox mechanism is still not complete. The intrinsic complexity of the NOE is due to the interdependence of multiple structural, chemical and electrochemical parameters that have been described in many papers, among which those written by Oliva et al. [5] and by McBreen [6] deserve a special mention. Perhaps the most controversial phenomenon is the so-called "second plateau" that corresponds to a partial transfer of the usual 1.2 V capacity to a 0.8-V potential plateau. Though many studies have been devoted to its study, the ultimate origin of this phenomenon is still unclear. Indeed, several explanations have been proposed in the literature. Among them are (i) an ohmic drop due to the formation of a barrier insulating layer at the active material/electron collector interface as deduced from the first electrochemical studies performed on this topic by Barnard et al. [7–9], (ii) the presence of another phase in the oxidized electrode, either γ-NiOOH as proposed by Sac-Epée et al. [10] from chemical/electrochemical experiments or Ni_2O_3H as proposed by Huggins from thermodynamic considerations on the ternary Ni–O–H system [11] or (iii) the existence of an insulating almost stoichiometric phase, $Ni(OH)_{2-\varepsilon}$, in the vicinity of the current collector, also deduced from chemical/electrochemical investigations performed by Léger et al. [12]. However, none of these explanations is completely satisfactory. On one hand (i) and (iii) fail to account for the amount of capacity delivered on the second plateau, contrary to hypothesis (ii) that correlated the amount of the second plateau to the amount of γ-NiOOH or Ni_2O_3H. But on the other hand, hypothesis (ii) is also dismissed

* Corresponding author. Tel.: +34 935801853x279; fax: +34 935805729.
E-mail address: rosa.palacin@icmab.es (M.R. Palacín).

0378-7753/$ – see front matter © 2008 Elsevier B.V. All rights reserved.
doi:10.1016/j.jpowsour.2008.01.045

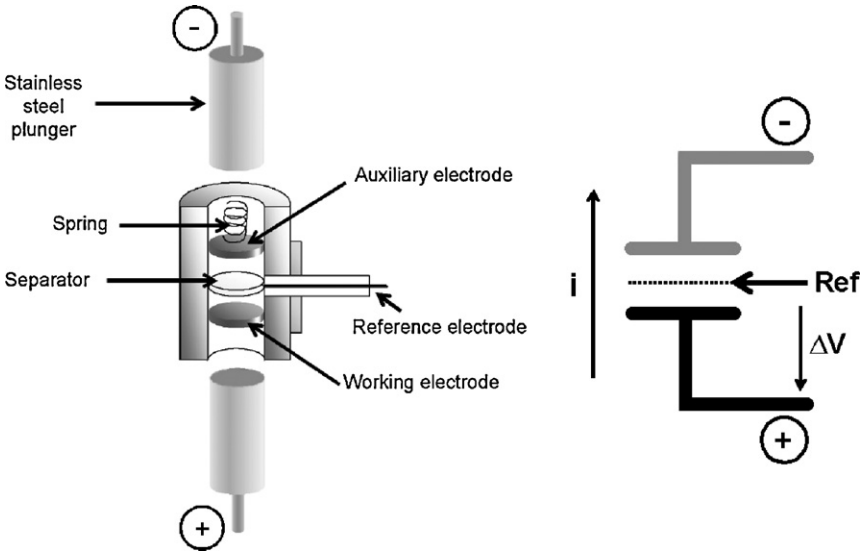

Fig. 1. Schematic view of the three-electrode T-Swagelock® cell.

by the fact that it has been confirmed that the second plateau can also be observed in the absence of the γ-NiOOH phase in the electrode and that no experimental report for the presence of black Ni_2O_3H [13,14] in the NOE has ever been found. We recently performed an *in situ* neutron powder diffraction study of the reduction process for NOE electrodes containing both β-NiOOH or γ-NiOOH [15] with different particle sizes, that allowed us to determine that the reduction process is similar in all cases and involves mainly a two-phase transformation during the whole reduction process along both the first and second plateau. The results of these studies coupled with PITT electrochemical experiments are a clear indication that the origin of the second plateau is not rooted on chemical phenomena as it does not arise from a phase transition or from an additional phase. Thus, its most probable origin is technological, probably the formation of a non-conducting layer as proposed by Barnard et al. in 1980 [7] the factors governing its amplitude being difficult to ascertain, as electrode technology involves many inter-related parameters.

With the aim of getting further insight in this problem we performed impedance spectroscopy measurements at different stages of reduction in order to follow its evolution. This is to our knowledge the first time that this technique is applied to the study of the second plateau, and the results obtained seem to indicate that in addition to the electronic contribution already pointed out by Barnard et al., ionic diffusion could also play an important role in the origin of this phenomenon.

2. Experimental

The impedance measurements were carried out using an Autolab Potentiostat 20 (Ecochemie, NL) coupled to a frequency response analyser. The impedance measurements were performed upon the reduction of the NOE: a constant current is applied for a certain time and then cut off to allow the electrode to relax. The impedance measurement was launched when the rest potential was becoming stable (e.g. not changing by more than few microvolt over 2 h). A sinusoidal voltage wave was then applied with a peak to peak value of 10 mV. The frequency range of the measurements was from 65 kHz to 20 mHz. All the measurements were carried out at 25 °C.

Three-electrode T-Swagelok® tight closed cells were used for impedance measurements (see Fig. 1). This type of configuration enables to work in limited amount of electrolyte (i.e. 0.05 mL), KOH 5 M. The auxiliary electrode was a disk cut from commercial $Cd/Cd(OH)_2$ electrode whereas the reference electrode was an oxidized silver wire. The working electrode was prepared by impregnating a nickel foam with a mixture of carbon SP/$Ni(OH)_2$/PTFE in a 30:65:5 mass ratio. The PTFE is used as a mechanical binder, and the carbon Super P as conducting additive. The pasted foam was dried at 55 °C, cut in disks of 12-mm diameter (1.15 cm^2) pressed at 2 tons cm^{-2} prior to use, that contained 21 mg of $Ni(OH)_2$ each. For simplicity the potential is expressed versus $Cd(OH)_2/Cd$. Cells were assembled in double and impedance measurements were carried out on the third reduction of one of them, once the proper working of the cell and the reproducibility of the results had been ensured. In addition to the experiments carried out in three-electrode cells, conventional cycling experiments were carried out using an Arbin potentiostat/galvanostat in similar two-electrode Swagelok® cells (i.e. without reference electrode). In all cases, the electrodes were oxidized at C/5 without overcharging in order to avoid the presence of γ-NiOOH in the electrode. The reduction rate was also C/5. At the end of charges and at the end of discharges the cell was allowed to relax for 10 min and 1 h, respectively.

X-ray powder diffraction measurements were performed on a Philips diffractometer PW1710 with Cu Kα radiation (λ = 1.54059 Å) whereas scanning electron microscopy micrographs were obtained using a Philips XL-30FEG. Specific surface areas were measured with a Micromeritics Gemini 2375 system according to the Brunauer–Emmet–Teller multipoint method by nitrogen physisorption at 77 K. The sample was previously dried under argon flow for 14 h and the free space was measured with helium gas at 77 K.

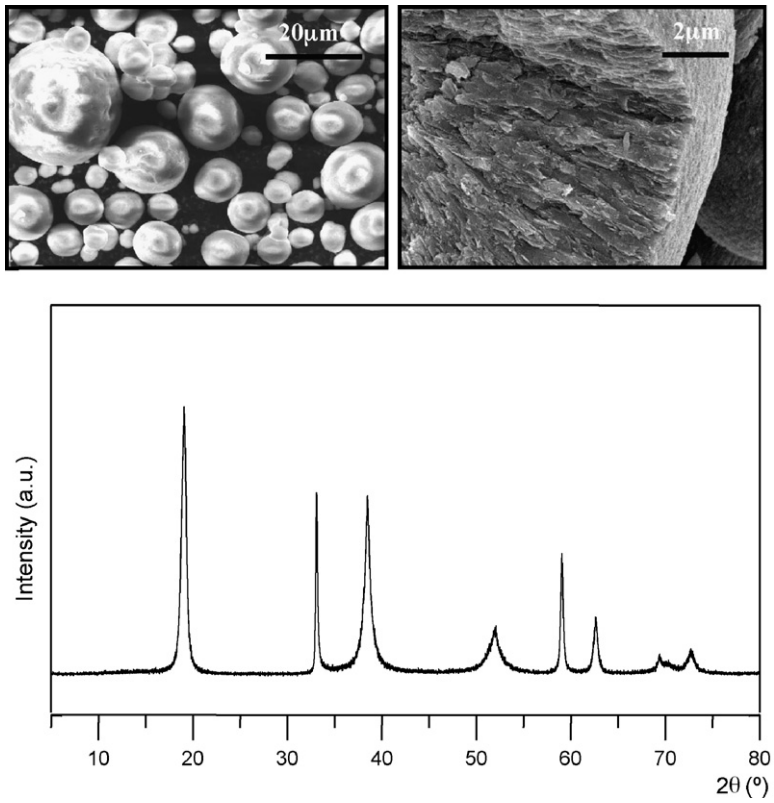

Fig. 2. X-ray diffraction pattern and typical SEM micrographs of the commercial $Ni(OH)_2$ sample used in this study.

Studies were carried out on a commercial $Ni(OH)_2$ consisting of spheres with a diameter between 5 μm and 20 μm, resulting from an agglomeration of thin platelets of nickel hydroxide of 250 Å of diameter with a BET surface of 16 $m^2\ g^{-1}$ (see Fig. 2).

3. Results and discussion

The conventional cycling experiments carried out confirm the expected behavior for non-cobalt-doped β-$Ni(OH)_2$ and a second plateau is observed upon reduction that accounts for about 20% of the total capacity. As the charge efficiency is not 100% due to the competing oxidation of water reaction, and to the fact that they were not subjected to overcharge to avoid the presence of γ-NiOOH at the NOE, the obtained capacities on reduction never attain one electron exchanged per formula unit and the values usually obtained are around 0.7 electrons. The three-electrode cells assembled for impedance measurements exhibited the same behavior (Fig. 3).

Fig. 4 shows the curve corresponding to the third reduction at C/5 rate of a NOE exhibiting the two successive plateaus at 1.25 V and 0.8 V versus $Cd(OH)_2$/Cd, respectively.

Impedance measurements were performed at different reduction levels. As seen in Fig. 4, a k index is used to point at which state the impedance measurement took place, so that the degree of electrode reduction increases with increasing k value. The electrode was first reduced up to the $k = 1$ marked point, then the current was interrupted and after potential stabilization an impedance measurement was carried out. This protocol was repeated until the last k-index, i.e. $k = 8$. By proceeding this way, it was possible to follow the impedance variation of the electrode while reduced.

In Fig. 5a and b the Bode diagrams of the impedance (modulus and phase angle as a function of frequency) for all the reductions levels are plotted.

The results clearly show that there are two main regimes: at high frequencies (above 100 Hz) the slope of the impedance curve is close to zero and the phase angle is lower than 5°; at low frequencies (below 100 Hz) there is a large variation of the impedance and of the phase angle as well. As the

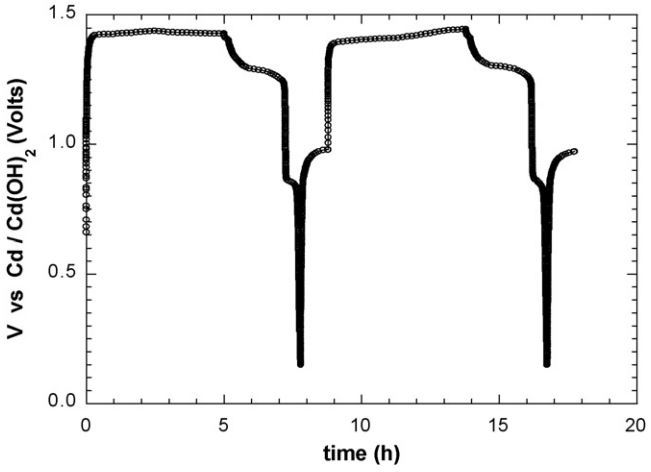

Fig. 3. Typical voltage vs. time profile for a NOE oxidized at C/5 and reduced also at C/5. The voltage evolution upon relaxation at the end of discharge confirms that the reduction process was fully completed.

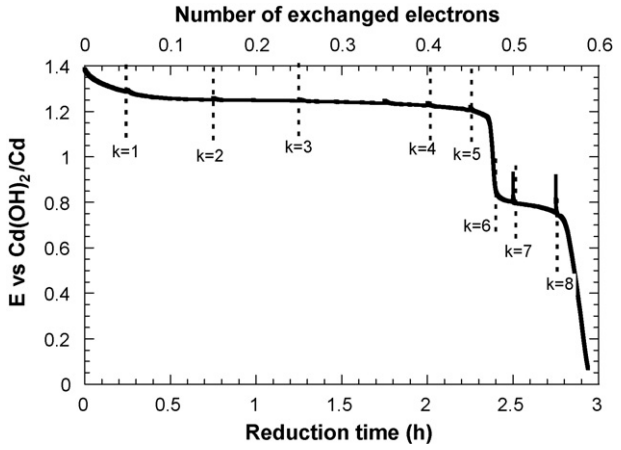

Fig. 4. Third reduction curve of a NOE electrode at C/5 rate in NaOH 5 M. At each k index an impedance electrochemical spectroscopy measurement was performed.

electrode is reduced three different consecutive behaviors are observed.

Between $k = 1$ and 3 (first plateau), both the phase angle and the impedance are more or less constant. At the end of the first plateau until the beginning of the second one ($k = 4$–7), the impedance increases sharply and varies linearly with $\log f$. Regarding the phase angle, it reaches rapidly a value as high as 85°. A maximum is observed after the transition from the first to the second plateau. When the second plateau begins ($k = 7$), there is a maximum at around 0.1 Hz followed by a slight decrease of the phase angle. Then, when the second plateau is completed ($k = 8$), a new situation is observed, the electrode is totally reduced and both the phase angle and the impedance decrease by several orders of magnitude.

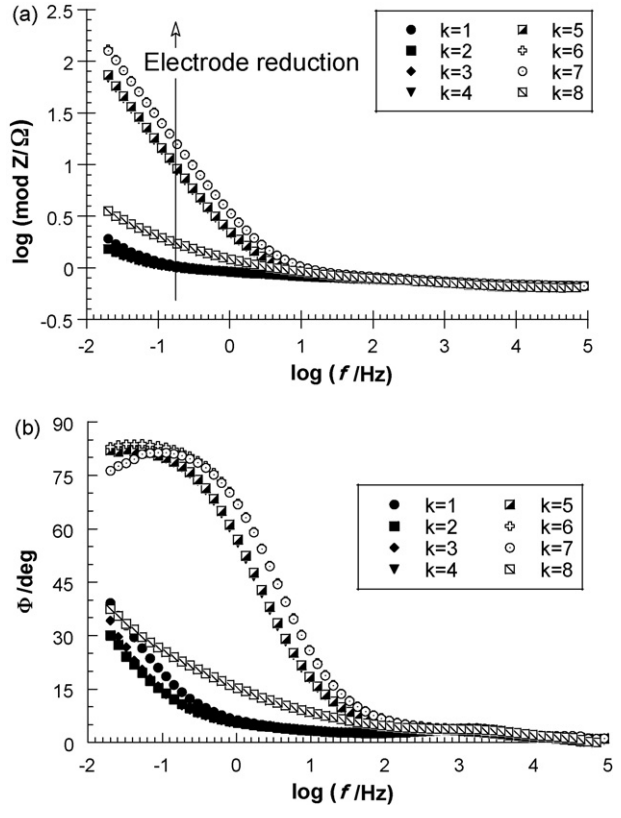

Fig. 5. Impedance modulus (a) and phase angle (b) corresponding to the measurements at different stages of reduction (see Fig. 4).

As the main magnitude variations in terms of impedance and phase angle occur at frequencies below 100 Hz, we focused our analysis in this frequency domain because the anomalous behavior of the NOE during reduction could be related to the large increase of impedance in this area. This is also consistent with the fact that numerous authors noticed that kinetics of nickel electrode are mainly governed by the transport of ions in the guest lattice, that is to say in the low frequency region [16–19]. Indeed, our results indicate that the NOE behaves as a blocking electrode as soon as the second plateau is approached. The fact that both the impedance modulus and the phase are low during the first plateau indicates that the electrochemical reaction

$$\beta\text{-NiOOH} + e + H^+ \rightarrow \beta\text{-Ni(OH)}_2$$

is achieved with a good efficiency. Previous *in situ* neutron diffraction studies along with PITT measurements [15] have clearly proved that the same electrochemical reaction occurs during the second plateau. However, the results of the impedance studies indicate that in this case the reaction is performed with poorer efficiency because both impedance and phase angle are much more higher than those observed during the first plateau.

Actually, a blocking behavior clearly appears during the transition between the first plateau and the second plateau. As mentioned previously, this phenomenon is noticed at low frequency, a fact that indicates that ionic transport is concerned. Nyquist plots of the first plateau ($k = 1$–3) show the typical expected behavior. First a high-frequency loop related to the double layer capacitance and the charge transfer resistance is observable and secondly a spatially restricted diffusion: a Warburg region followed by a more capacitive region. This type of behavior is typical of an active material layer on a metallic substrate. The small deviations observed for the Warburg and restricted diffusion regions can be attributed to the porosity of the electrode. Regarding the Nyquist plot of the second plateau, the blocking electrode behavior is observed, that could be caused by the existence of a poor conductive film between the electrode and the electrolyte. Nevertheless, a parallel leak resistance subsists and diminish when the second plateau starts ($k = 7$), that could be related to the existence of an ionic path across the insulator layer. The magnification of the high-frequency zone shows that the charge transfer loop remains but with a smaller amplitude and is almost masked by the low-frequency capacitance.

As referred in previous works [20,21] the reduction reaction takes place at the interface between NiOOH and the electrolyte. Fig. 7 shows a simple sketch illustrating this behavior.

To attempt to render the porosity effect, a unique pore model was adopted. Needless to say that in a real electrode the model could be more complicated due to the nature of the electrode. The electrode is made of compacted active material grains that lead to a large specific surface. But the model presented is sufficient to give a good understanding on the phenomena that could occur during the electrode reduction.

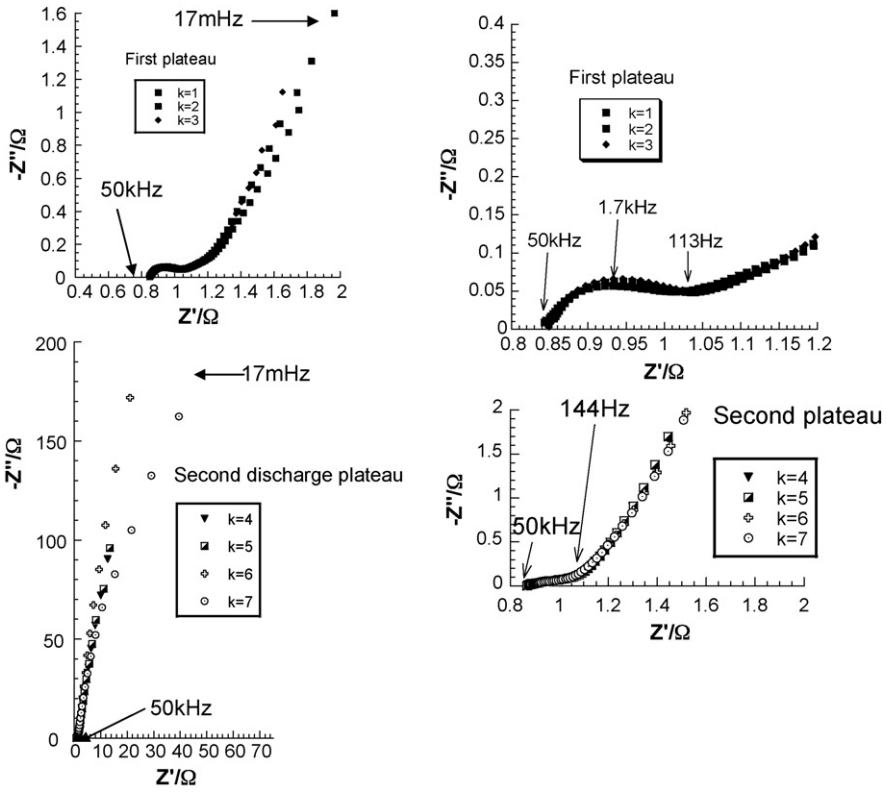

Fig. 6. Nyquist plots and different high frequency zooms.

The process can be described assuming three different stages of the electrode depending directly on the state of charge. First stage is linked to the k index number one (see Fig. 4), the active material is more or less NiOOH (stage 1) and even if a part of $Ni(OH)_2$ had covered a part of the electrode surface a large amount of NiOOH is not covered. That means that there is a direct contact of the NiOOH with the liquid electrolyte. Fig. 6 also clearly shows that for $k = 1$ the Nyquist plot is that of a porous film soaking in a liquid electrolyte. During reduction, the electronic insulating layer of $Ni(OH)_2$ continues to grow (Fig. 7, stage 2). It is more and more difficult for the protons to reach the electrochemical sites and lead to an increase in the diffusion impedance. The Nyquist plot for $k = 5$ shows that at the end of the first plateau this impedance tends to be mainly capacitive. Upon NOE reduction the $Ni(OH)_2$ is building up and when the whole active material surface is covered (Fig. 7, stage 3) the protons have to push their way through the $Ni(OH)_2$ layer. Figs. 5 and 6 for $k = 7$ show that the electrode/electrolyte interface is blocking and that a small drop of phase angle could be related to the leak resistance at this interface due to the ionic migration of the proton through the $Ni(OH)_2$ electronic insulating layer.

In other words, the active material continues its reduction through the ionic resistance of nickel hydroxide layer. This situation is analogous to a replacement of the liquid electrolyte by a solid electrolyte.

Two different regimes should be then considered for the whole reduction process: one, during the first plateau, is governed by diffusion from the electrolyte to the active material surface; the other, during the second plateau, is controlled by the proton diffusion through the hydroxide layer at the surface of the active material. These simplistic sketches show that a critical thickness of the insulating layer of $Ni(OH)_2$ could be defined that involves the reduction of a certain amount of NiOOH. Over this point, the reduction goes on but with the high voltage drop cor-

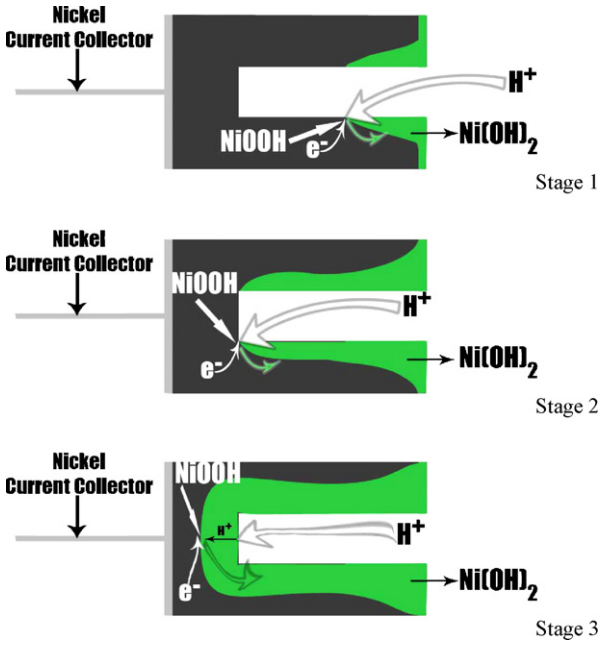

Fig. 7. Schematics of the NOE reduction process.

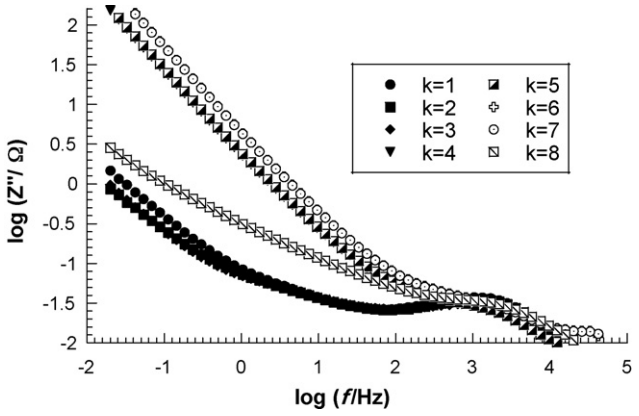

Fig. 8. Imaginary part of the impedance as function of the frequency.

responding to the second plateau and continues then through the insulating layer.

The diffusion impedance can be described by a well-known general exponent law which generalises the so-called Warburg impedance and which is most of time called CPE (constant phase element):

$$Z_D(j\omega) = \frac{1}{Y_0}(j\omega)^{-\alpha} \quad (0 < \alpha < 1) \tag{1}$$

Z_D is the diffusion impedance, α is an exponent depending both on diffusion regime and dispersions induced by the porosity of the electrode and Y_0 constant phase element modulus ($F{\cdot}s^{1-\alpha}$). Commonly, two particular values can be emphasized, one when $\alpha = 1/2$ and the other when $\alpha = 1$. Basically, the diffuse layer is described by this equation:

$$\delta = \sqrt{\frac{D}{\omega}}$$

δ is the diffusive length that is, to say, the mean-free path per cycle, whereas D is the apparent diffusion coefficient of the proton involved during the reduction process of NiOOH. If the thickness of active material (e) is taken as a characteristic length, it means that at high frequency, i.e. $\delta \ll e$, the semi-infinite Warburg law applies and $\alpha = 1/2$. On the other hand, at low frequency, i.e. $\delta = e$, restricted diffusive mode occurs and the electrode behaves like a capacitor, $\alpha = 1$. Needless to say that this is a very simple case and some deviations are expected due, for instance, to the porosity of the electrode. To extract α with a better accuracy, a $\log Z''$–$\log f$ plot is used because the resistive part can attenuate the slope changes. As defined by Eq. (1) $\log Z''$ varies linearly with $\log f$ and the value of the slope is α. Fig. 8 represents the imaginary part of the impedance variation with frequency. For the already explained reasons, we have mainly focused on the low-frequency behavior, i.e. $f < 100$ Hz.

Slope values measured from Fig. 8 are reported in Table 1. From $k = 1$ to 3, the NOE is reduced on the first plateau and two slopes are observed. This is an expected behavior, since diffusion processes on such porous electrode usually take place in two successive regimes: first with a semi-infinite Warburg region and then a more capacitive zone appears as the frequency

Table 1
Values of α at high (HF) and low (LF) frequencies extracted from the plot in Fig. 8

k	α_{HF}	α_{LF}	Correlation coefficient
1	0.26	0.69	>0.99
2	0.24	0.62	>0.99
3	0.23	0.70	>0.99
4	–	0.89	>0.99
5	–	0.91	>0.99
6	–	0.91	>0.99
7	–	0.90	>0.99

of the signal is decreasing. This phenomenon is well known and directly related to the diffusion boundary conditions in a porous electrode, i.e. $C_{H^+,bulk} = C^\circ$ and $(dC/dx)_{x=0} = 0$ [22] Thus, average values of 0.25 and 0.7 are measured for $k = 1$–3, instead of theoretical 0.5 and 1, due to the porosity of the electrode. These measurements show that during the first plateau proton reaches the active material directly from the electrolyte. When the reduction proceeds ($k = 4$–7) a poorly conductive layer of $Ni(OH)_2$ hinders more and more the ionic motion. As explained earlier in this paper, to access the remaining active layer protons have to get through the $Ni(OH)_2$ layer so that the mass transport gets more kinetically limited and the NOE tends to a capacitive behavior with an average slope of 0.9 being obtained from Z''plot. In this case, the remaining NiOOH and the electrolyte stand for the armature of the capacitor and the $Ni(OH)_2$ for the dielectric and proton diffusion leads to the leak resistance previously noticed on capacitance plots. It can be seen that, as compared to the first stages ($k = 1$–3), the α deviation from theoretical value is very low (0.9 against 1), which is consistent with the hypothesis that a compact layer of $Ni(OH)_2$ is formed without significant porosity.

The results obtained from impedance spectroscopy are in agreement with neutron diffraction, PITT [15] and also with previous GITT measurements [23] that give clear proof that the equilibrium voltage is the same during the first and second plateaus. Thus it seems clear that rather than having a chemical origin, the second plateau is related to the formation of a barrier layer at the interface that would not only be electronically insulating as already pointed out by Barnard et al. [7–9] but would also hinder ionic diffusion.

4. Conclusions

Electrochemical impedance spectroscopy was applied to the study of the second plateau occurring during the reduction of the NOE. The results show that a large variation of impedance appears when the NOE goes from the first to the second plateau. The variation takes place mainly at low frequencies related to ionic diffusion. We observe that the impedance becomes more capacitive at the second plateau meaning that proton diffusion is restricted. These results would be consistent with the formation of an insulating layer of nickel hydroxide at the interface between the NOE and the electrolyte during reduction that would hinder not only electronic but also ionic conduction. The voltage drop observed upon transition to the second plateau would

occur once this layer becomes compact and the ionic diffusion is forced to occur through the layer.

Acknowledgements

We are grateful to Y. Chabre, A. Delahaye-Vidal, M. Dollé and C. Maugy for helpful discussions and to M. Dollé for his help with the realization of the impedance measurements.

References

[1] W. Jungner, Swedish Patent 15,567 (1901).
[2] W. Jungner, German Patent 163,170 (1901).
[3] T.A. Edison, German Patent 157,290 (1901).
[4] T.A. Edison, US Patent 678,722 (1901).
[5] P. Oliva, J. Leonardi, J.F. Laurent, C. Delmas, J.J. Braconnier, M. Figlarz, F. Fievet, A. de Guibert, J. Power Sources 8 (1982) 229–255.
[6] J. McBreen, Modern Aspects of Electrochemistry, vol. 21, Plenum Press, New York, 1990, pp. 29–63.
[7] R. Barnard, G.T. Crickmore, J.A. Lee, F.L. Tye, J. Appl. Electrochem. 10 (1980) 61–70.
[8] R. Barnard, C.F. Randell, F.L. Tye, J. Appl. Electrochem. 10 (1980) 109–125.
[9] R. Barnard, C.F. Randell, F.L. Tye, J. Appl. Electrochem. 10 (1980) 127–141.
[10] N. Sac-Epée, M.-R. Palacin, B. Beaudoin, A. Delahaye-Vidal, T. Jamin, Y. Chabre, J.-M. Tarascon, J. Electrochem. Soc. 144 (11) (1997) 3896–3907.
[11] R.A. Huggins, Solid State Ionics 177 (26–32) (2006) 2643–2646.
[12] C. Léger, C. Tessier, M. Ménétrier, C. Denage, C. Delmas, J. Electrochem. Soc. 146 (3) (1999) 924–932.
[13] C. Greaves, A.M. Malsbury, M.A. Thomas, Solid State Ionics 18/19 (1986) 763–767.
[14] A.M. Malsbury, C. Greaves, J. Solid State Chem. 71 (2) (1987) 418–425.
[15] F. Bardé, M.R. Palacín, Y. Chabre, O. Isnard, J.M. Tarascon, Chem. Mater. 16 (2004) 3936–3948.
[16] L. Xiao, J. Lu, P. Liu, L. Zhuang, J. Yan, Y. Hu, B. Mao, C. Lin, J. Phys. Chem. B 109 (2005) 3860–3867.
[17] L. Xiao, J. Lu, P. Liu, L. Zhuang, J. Phys. Chem. B 110 (2006) 2057–2063.
[18] S. Deabate, F. Fourgeot, F. Henn, Electrochim. Acta 51 (2006) 5430–5437.
[19] J. Bisquert, Electrochim. Acta 47 (2002) 2435–2449.
[20] R.A. Huggins, H. Prinz, M. Wohlfahrt-Mehrens, L. Jörissen, W. Witschel, Solid State Ionics 70/71 (1994) 417–424.
[21] V. Mancier, P. Willmann, A. Metrot, J. Power Sources 85 (2000) 181–185.
[22] J. Bisquert, G. Garcia-Belmonte, F. Fabregat-Santiago, P. Roberto-Bueno, J. Electroanal. Chem. 475 (1999) 152–163.
[23] N. Sac-Epée, M.R. Palacín, A. Delahaye-Vidal, Y. Chabre, J.M. Tarascon, J. Electrochem. Soc. 145 (5) (1998) 1434–1441.